How Much π-Stacking Do DNA Termini Seek? Solution Structure of a Self-Complementary DNA Hexamer with Trimethoxystilbenes Capping the Terminal Base Pairs[†,‡]

Jennifer Tuma,[⊥] Ralph Paulini,[§] Jan A. Rojas Stütz,[#] and Clemens Richert*[,#]

Max-Planck-Institute for Biophysical Chemistry, D-37077 Göttingen, Department of Chemistry, University of Konstanz, D-78457 Konstanz, and Institute for Organic Chemistry, University of Karlsruhe (TH), D-76131 Karlsruhe, Germany

Received August 19, 2004; Revised Manuscript Received October 2, 2004

ABSTRACT: The exposed terminal base pairs of DNA duplexes are nonclassical binding sites for small molecules. Instead, small molecules usually prefer intercalation or minor groove binding. Here we report the solution structure of the DNA duplex (TMS-TGCGCA)$_2$, where TMS denotes trimethoxystilbene carboxamides that are 5′-tethered to the DNA. The stilbenes, for which intercalation is conformationally accessible, stack on the terminal T:A base pairs of an undisturbed B-form duplex. Two conformations, differing by the orientation of the stilbene relative to the terminal base pair, are observed, indicating that the flip rate is slow for the π-stacked aromatic ring system. The trimethoxystilbene is known to greatly increase base pairing fidelity at the terminus. Here we show that it gauges the size of the T:A base pair by embracing the 2′-methylene group of the terminal dA residue of the unmodified terminus with its methoxy "arms", but that it does not engage the entire base pair in π-stacking. Mismatched base pairs with their altered geometry will not allow for the same embracing interaction. On the basis of the current structure, a trimethoxychrysene carboxamide is proposed as a ligand with increased π-stacking surface and possible applications as improved fidelity-enhancing element.

Small molecules usually bind DNA via one of three possible modes of binding: intercalation, minor groove binding, and external binding to the backbone, driven by electrostatic interactions (*1*). A fourth binding mode is accessible, though, which may be termed "capping" (Figure 1). This form of binding involves the plane of the otherwise exposed terminal base pair as the binding site for small hydrophobic molecules. While binding to termini has been difficult to study with polymeric DNA from natural sources, the availability of defined short sequences via automated DNA synthesis has made possible the exploration of capping as a binding mode. Capping can be favored by covalently tethering the small molecule to one or both termini of DNA duplexes. Recent examples of oligonucleotide duplexes thus modified that have yielded high-resolution structures that show capping include doubly tethered stilbenediethers (*2*, *3*), a phenazinium moiety capping a DNA:RNA duplex (*4*), a tryptophan as 5′-acylamido substituent of a DNA duplex with dangling residues (*5*), and a cholic acid residue capping a duplex with blunt ends (*6*).

Understanding what drives binding to the termini is important because many key biochemical processes, such as replication, certain repair processes, degradation by exonucleases, and gyrase-induced supercoiling, all involve steps occurring at the interface between a terminus and a (protein) ligand. Further, the terminus is interesting for a fundamental reason, as it provides a planar surface where π-stacking interactions (*7*) can be studied that are more extensive than usual in folded biomacromolecules. Finally, capping the termini is a novel approach for increasing the base pairing fidelity of hybridization probes (*8*). Other approaches that involve small molecule ligands have been developed for PCR[1] primers (*9*). Without caps that selectively stabilize canonical base pairs, mismatches at the termini induce little destabilization (*10*), probably due to unrestricted fraying and wobbling.

Among the small molecule ligands that can show capping when tethered to the termini, stilbenes have attracted significant attention, since they can be used to study electron transfer in DNA (*11*−13). But certain stilbenes are also known as DNA-binding molecules in their own right. Some of them can have biological activity (*14*, *15*). A recent study on a range of substituted stilbenes has led to the identification of the 3,4,5-trimethoxystilbene-4′-carboxamidopropanol phosphate group as a fidelity-enhancing element for hybridization probes that induced UV melting point differences between

[†] This work was supported by DFG (Grant No. 1063/1-3) and Fonds der Chemischen Industrie (project 164431). The NMR laboratory at the Institute of Organic Chemistry at U. Karlsruhe is supported by an HBFG grant (Gz. 158-380). J.T. was a predoctoral fellow of the State of Baden-Württemberg.

[‡] Coordinates of two structures, representative of either conformation found, have been deposited in the RCSB Protein Data Bank (entry ID 1X6W).

* To whom correspondence should be addressed. Tel. int.-49 (0) 721 608 2091; fax int.-49 (0) 721 608 4825; e-mail: cr@rrg.uka.de.

[⊥] Max-Planck-Institute for Biophysical Chemistry.

[§] University of Konstanz.

[#] University of Karlsruhe (TH).

[1] Abbreviations: TMS, trimethoxystilbene residue; PCR, polymerase chain reaction; NOESY, nuclear Overhauser enhancement spectroscopy; DQF-COSY, double quantum-filtered correlation spectroscopy; TOCSY, total correlation spectroscopy; MALDI-TOF MS, matrix-assisted laser desorption ionization time-of-flight mass spectrometry.

10.1021/bi048205y CCC: $27.50
Published on Web 11/23/2004

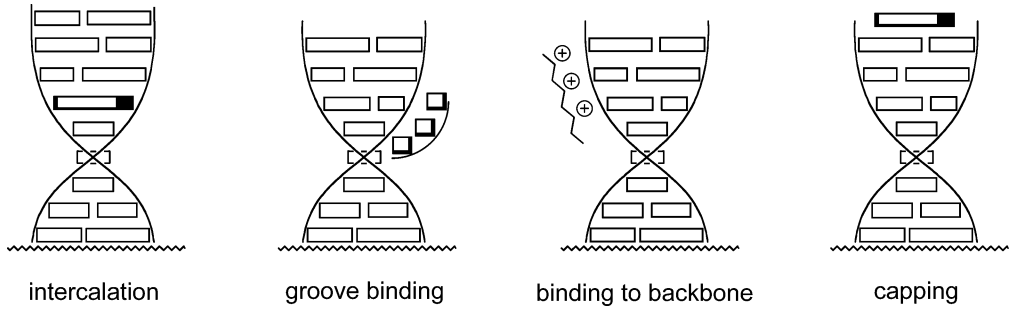

FIGURE 1: Binding modes for small molecules interacting with DNA duplexes.

fully matched duplexes and duplexes with a single terminal mismatch of up to 23.4 °C (*16*). The fidelity-enhancing effect of the trimethoxystilbene is greater than that of pyrene derivatives (*10*), even through pyrene offers more surface area and should thus engage in stronger stacking interactions. The fidelity-enhancing effect is also stronger than that of a steroid that had previously been shown to fit exquisitely onto terminal base pairs (*6*, *8*).

The observation that the trimethoxystilbene substituent is more duplex-stabilizing than stilbene substituents with electron-withdrawing substituents was unexpected. The electron-rich distal ring of the alkoxystilbene could be expected to stack on the purine ring system of the deoxyadenosine residue found at the 3′-terminal position of the target strand. This would place two electron-rich π-systems on top of each other, which should be energetically less favorable than stacking between an electron-depleted and an electron-rich ring system. The available high- and low-resolution structures of DNA duplexes with stilbenes covalently tethered to both termini (*2*, *3*) did not provide clues that helped to explain this phenomenon. Instead, the former shows a surprising structural heterogeneity, in that the stilbene ring system in these hairpins binds to the neighboring DNA base pair both in the usual π-stacking arrangement and in an edge-on or T-shaped arrangement (*3*). This prompted us to study the structure of trimethoxystilbene-tethered complexes by NMR and restrained molecular dynamics.

Here we report the solution structure of a DNA duplex with trimethoxystilbenes bound to the termini. This duplex shows how the trimethoxystilbene can gauge the shape of the base pair with their alkoxy substituents, thus explaining the exceptional fidelity-enhancing effect of this substituent on the base pairing at the termini of hybridization probes (*16*). The NMR results also show structural heterogeneity, with a second conformation detectable both in the one- and two-dimensional data and the molecular dynamics results.

MATERIALS AND METHODS

Sample Preparation and NMR Spectroscopy. The synthesis of the DNA portion of **1** was performed on a Perseptive Biosystem 8909 Expedite DNA synthesizer using β-cyanoethyl phosphoramidites and the standard protocol for 3 μmol scale syntheses, as recommended by the manufacturer. DNA synthesis reagents were from Proligo (Hamburg, Germany). Samples of 94 mg (3 μmol loading) of controlled pore glass (cpg-dA^{Bz}) with 1000 Å pore size were used in polypropylene reaction chambers for DNA synthesis (Prime Synthesis, Aston, PA). The coupling step installing the stilbene residue employed (*E*)-3,4,5-trimethoxyphenylvinyl benzocarbonylaminopropyl-1-*O*-cyanoethyl-*N*,*N*-diisopropylphosphoramidite (*16*) (171 mg, 300 μmol) in dry acetonitrile (150 μL), the same volume of activator solution, an extended coupling time of 30 min, and was repeated once before oxidation to ensure complete conversion. The product was released by treatment with ammonium hydroxide (30% aqueous NH_3, 3 mL) for 16 h at 25 °C. Excess ammonia was then removed with a gentle air stream directed onto the surface of the solution for 1 h. The supernatant was aspired, and the support was washed with deionized water (2 × 0.7 mL). The combined aqueous solutions were filtered (0.2 μm pore size, Whatman Inc) and used directly for HPLC on a 250 × 10 mm Nucleosil 300-7 C4 column (Macherey-Nagel, Düren, Germany), with a gradient of CH_3CN in 0.1 M triethylammonium acetate, pH 7 (0% for 5 min, to 27% in 30 min, elution at 32 min), at a flow rate of 3 mL/min and detection at 260 nm. The purified product was lyophilized from water (3 × 0.75 mL), 10% aqueous NH_3 (4 × 0.75 mL) and D_2O (2 × 0.5 mL). Yield 0.57 μmol (19%, based on cpg-dA^{Bz} loading), intensity of product peak in the HPLC trace of the crude: 79%. MALDI-TOF MS (linear, negative mode, trihydroxyacetophenone/diammonium citrate matrix) calcd for $C_{79}H_{97}N_{24}O_{41}P_6$ ([M−H]$^-$) 2224.5, found 2226.2; UV−vis (H_2O, qualitative) λ_{max} (nm) 255 (100%), 335 (41%); ϵ_{260} (calc) 73 000 M^{-1} cm^{-1}.

Samples were dissolved in 200 μL of D_2O or H_2O/D_2O (9:1) containing 150 mM NaCl and 10 mM phosphate buffer, pH 7 (uncorrected for deuterium effect). The solution containing 90% H_2O was employed for experiments detecting exchangeable protons. NMR spectra were recorded in NMR microtubes susceptibility-matched to D_2O (Shigemi Co., Tokyo, Japan) on Bruker spectrometers with 600 or 800 MHz ^{1}H resonance frequencies at a temperature of 288 K. Two-dimensional spectra were acquired with 2048 data points in f2 and 512 or 256 increments in f1. The HDO peak in spectra from D2O solutions was suppressed via presaturation during the recycle delay. For the samples in H_2O/D_2O, the WATERGATE pulse sequence (*17*) was employed. NOESY spectra were acquired at mixing times of 100, 250, 300, and 500 ms. Further, DQF-COSY and TOCSY spectra were acquired to aid the assignment, the latter with a spin lock time of 70 ms. Processing and analysis of the NMR spectra were performed in XWINNMR (Bruker Biospin).

Assignments. Resolved resonances belonging to the major conformation (conformation 1) or the minor conformation (conformation 2) could be identified based on their relative intensities (4:1). For conformation 1, an uninterrupted series of NOESY cross-peaks connecting H1′ and nucleobase resonances allowed for the sequential assignment (*18*−20)

of anomeric and nonexchangeable nucleobase resonances. The chemical shift of the methyl group of T2 was assigned on the basis of the NOESY cross-peak to H6 of the same residue and provided the starting point for the sequential assignment. On the basis of the resonances of the H1′ protons, the chemical shifts for protons of the individual spin systems were identified in DQF-COSY and TOCSY spectra. The assignments were confirmed in NOESY spectra. The stilbene spin system of the proximal ring was identified in the DQF-COSY spectrum. Both the protons of the olefinic bridge and those of the methoxy-substituted distal ring are isochronous and appear as singlets. The identity of the respective singlets was established based on the intensity of NOESY cross-peaks to the methyl groups of the methoxy substituents. The resonances of the methylene units of the propyl chain of the linker were assigned based on NOESY cross-peaks to the stilbene moiety and COSY connectivities. Assignment of the resonances of conformation 2 followed the same principles. The chemical shift differences between the respective resonances in the major and minor conformation were greatest for the stilbene ring system and decreased toward the interior of the duplex. Full assignments are given in the Supporting Information.

Generation of Restraints. For the generation of distance restraints, NOESY spectra recorded at a mixing time of 300 ms were used. Cross-peaks in NOESY spectra acquired in D_2O were integrated using XWINNMR. On the basis of the intensity of cross-peaks between protons of known distance, such as H5 and H6 of dC residues, NOESY cross-peaks were divided into very strong (interproton distance of 2.5 Å), strong (3.0 Å), medium (3.5 Å), weak (4.0 Å), very weak (4.5 Å), and very very weak (5.0 Å) signals. The distances were used as constraints with boundaries of ±1.0 Å. In the case of overlapping peaks or peaks showing substantially different intensity on the two sides of the diagonal, boundaries of ±2.0 Å were used. Pairs of protons from the stilbene that were isochronous were treated with the pseudoatom approach, using the averaging function for distance restraints and the setting "sum" in X-PLOR (version 3.851) (*21*). Pairs of diastereotopic protons from deoxyribose residues not assigned individually, such as certain H5′/5″ protons, were treated with the geometric center pseudoatom approach of X-PLOR.

Since the chemical shift of the imino protons of deoxyguanosine and thymidine residues appear in the region typical for hydrogen bonding in Watson−Crick base pairs in spectra acquired in H_2O/D_2O (9:1), base pair constraints (hydrogen bonding and base-pair planarity) were introduced, using the default values of CNS (version 1.0) (*22*) with constraint boundaries of 0.1 Å for the hydrogen bonds. The NOESY peaks between protons of neighboring nucleotides are those expected for an undisrupted B-form duplex (*23*). Further, the H1′ protons of the nucleotides appear as triplets, with $^3J(1'2')$ coupling constants of 6.5−8.0 Hz, as expected for B-form DNA. Consequently, dihedral angle constraints for B-form DNA from the literature (*24*) were used for the backbone angles with boundaries of ±20°.

Structure Generation and Restrained Molecular Dynamics. Topology and parameter files for the molecular dynamics calculation of $(\mathbf{1})_2$ were generated on the basis of X-PLOR files for DNA. For the stilbene residue, parameters were generated with the help of XPLO2D (*25*), based on an X-ray crystal structure (*26*). The link between the stilbene residue and the modified thymidine was created using the generate.inp file of X-PLOR. Restrained molecular dynamics calculations were carried out in CNS (*22*) with the torsion angle molecular dynamics protocol (*27*). The details of the protocol are the same as those used in earlier work from our laboratory (*6*). Trivial cross-peaks, expected independent of conformation, based on the covalent structure, were not entered to improve the efficiency of the algorithm. During refinement, restraint violations were detected using VMD-XPLOR (*28*). Minimizing them by comparison of experimental and back-calculated NOESY spectra was one key strategy for obtaining improved structures. Back-calculated spectra were generated in GIFA (*29*) and the cross-peaks intensities back-calculated with X-PLOR using the two-spin approximation. Data on the restraints used and the quality of the structures obtained are compiled in Table 1. The coordinates of representative refined structures of $(\mathbf{1})_2$ have been deposited in the PDB database. The PDB ID code is 1X6W.

Table 1: Constraints Used for Molecular Dynamics and Quality of Structure Obtained

Constraints	
NOE-based constraints (total)	104
interresidue	12
intraresidue	92
dihedral angle constraints	32
hydrogen bonding constraints	16
base pair planarity constraints	6
Data on the 15 Lowest Energy Structures	
restraint violations	
NOE violation > 0.5 Å	0
dihedral angle violation > 30°	0
deviation from ideal geometry	
bond distances > 0.05 Å	0
bond angles > 5.0°	0
Refinement Statistics for 15 Lowest Energy Structures	
rmsd from average (all coordinates)	1.09 Å
(backbone)	0.59 Å
pairwise rmsd (all coordinates)	1.59 Å
(backbone)	0.88 Å
energy	−382 ± 6 kcal/mol

RESULTS

The sequence of $(\mathbf{1})_2$, the DNA duplex studied in this work, is shown in Figure 2. This duplex has previously been shown to have a UV-melting point up to 22.3 °C higher than that of unmodified $(TGCGCA)_2$ (*16*). It consists of a mixed sequence, self-complementary hexamer with a core of four C:G base pairs and terminal A:T base pairs, which can easily be disturbed by substituents that favor refolding (*30*). The one-dimensional ^1H NMR spectrum of $(\mathbf{1})_2$ shows more than one set of signals (Figure 3). The available spectroscopic and chromatographic data, including MALDI-TOF MS, UV−vis spectroscopy, and HPLC show a single, pure compound. Accordingly, it was assumed that $(\mathbf{1})_2$ adopts more than one conformation, and that the interconversion between these conformations is slow on the NMR time scale. Integration showed a ratio between the predominant set of signals and the less intense one of 4:1. A few isolated signals from a presumed third set of signals with very low intensity can also be discerned (Figure 3). These did not allow for meaningful assignment work. A sufficient number of signals

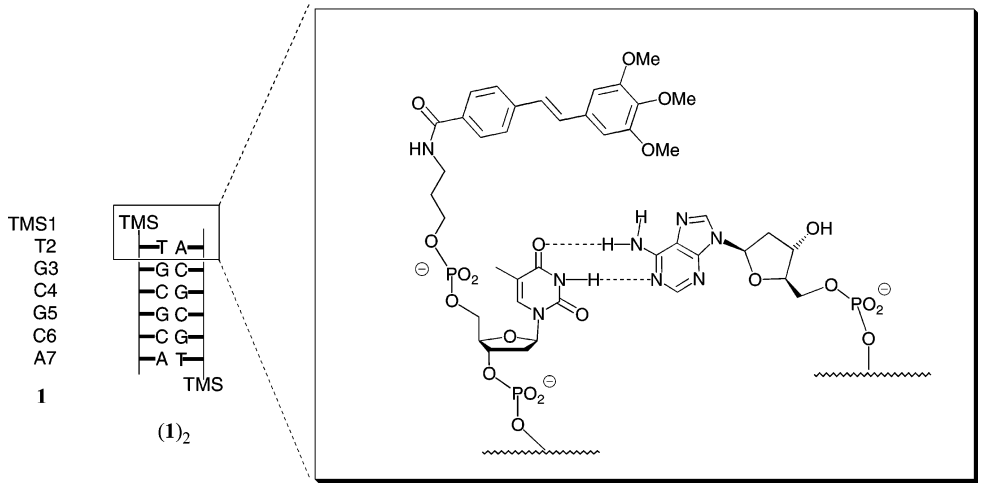

FIGURE 2: Sequence of the duplex studied. The box on the right-hand side shows details from the terminus.

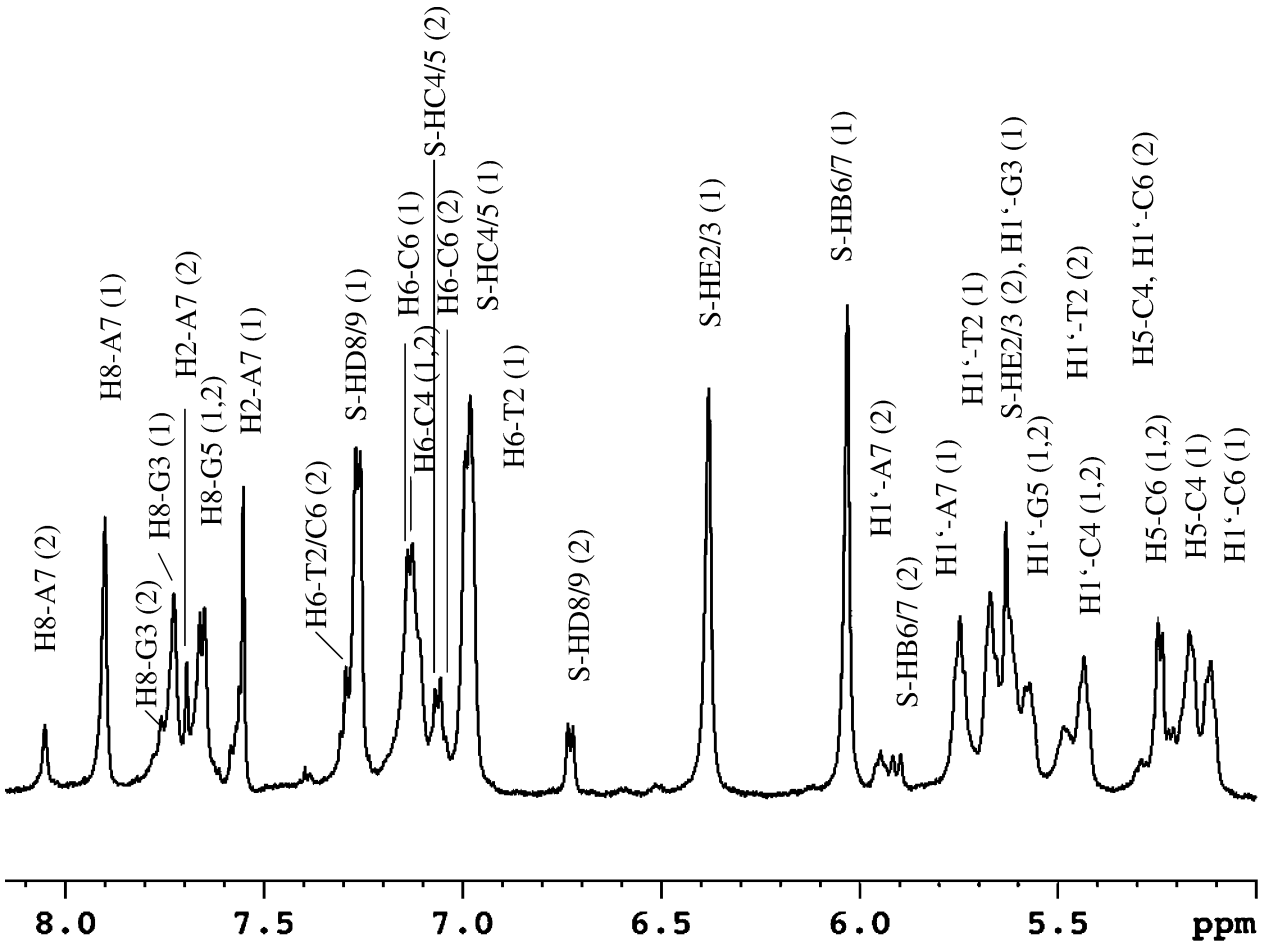

FIGURE 3: Low field region of the one-dimensional ^{1}H NMR spectrum of $(\mathbf{1})_2$ at 600 MHz in D_2O, 150 mM NaCl, and 10 mM phosphate buffer, at 600 MHz, and 288 K. Peak assignments for the major conformation (1) and the minor conformation (2) are shown.

was nonoverlapping for the two prominent conformations, though, which will subsequently be referred to as conformation 1 and conformation 2.

Peak assignment for conformation 1 (major conformation) was achieved using conventional approaches, as detailed in the experimental part. The anomeric protons and the H6/8 protons of the nucleobases show NOESY cross-peaks typical for B-form DNA duplexes (Figure 4). The H1′ proton resonances identified in NOESY spectra provided the starting points for assignments in the deoxyribose spin systems via DQF-COSY and TOCSY cross-peaks. The remaining prominent peaks were assigned to the stilbene substituents, although more isochronous resonances were observed than initially expected. The assignment of the resonances of conformation 2 followed the same principles.

The proton chemical shifts for the stilbene and the terminal nucleotides are quite different for the two conformations but become increasingly similar toward the interior of the duplex. This suggested that it is the termini where the two differ the most in their “folding”. Entering loosely defined distance constraints based on NOESY cross-peaks from both sets of resonances gave families of structures that differed in the

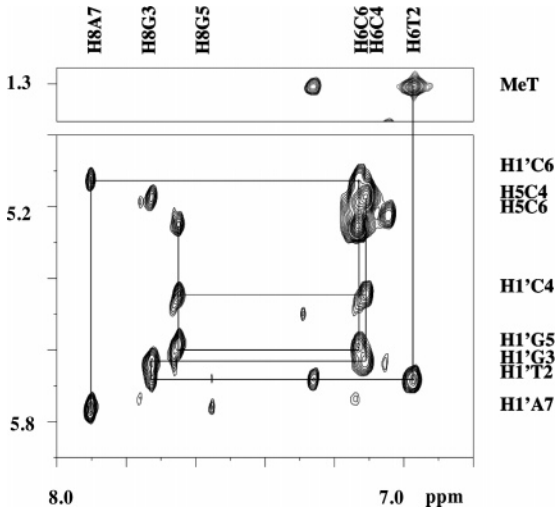

FIGURE 4: Expansion of the NOESY spectrum of $(\mathbf{1})_2$ in D_2O, phosphate buffered saline at 288 K and 300 ms mixing time. Cross-peaks between H-1′ and nucleobase resonances are shown and the sequential assignment is indicated by lines.

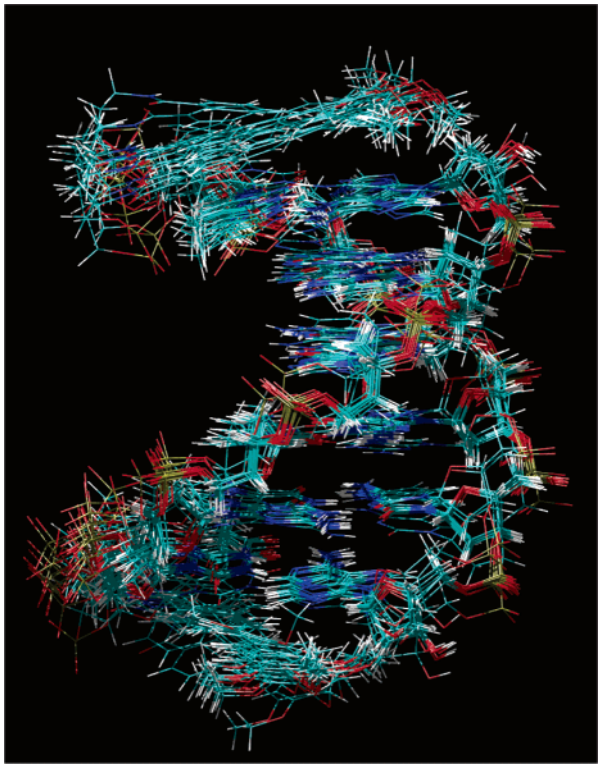

FIGURE 5: Overlay of 15 structures of lowest energy, as obtained for $(\mathbf{1})_2$ by restrained molecular dynamics.

orientation of the stilbene ring system relative to the terminal base pair. Refinement led to satisfactory convergence in the structures calculated by torsion angle molecular dynamics (*27*), as shown in Figure 5. Among the 15 duplexes of lowest energy obtained through molecular dynamics, eight show conformation 1 at both termini, three show conformation 1 at one terminus and conformation 2 at the other, and two show conformation 2 at both termini. Thus, the ratio of termini showing conformation 1 versus 2 (19:7) roughly agrees with the relative intensity of the ^{1}H NMR signals for the two sets of signals (4:1).

No cross-peaks between the stilbene and nucleobases other than those of the terminal base pair were observed in the

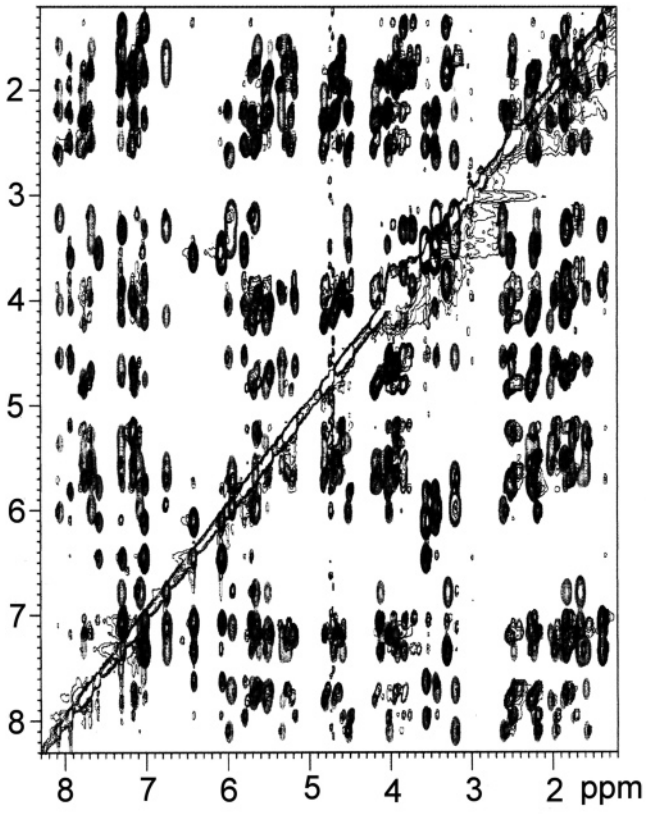

FIGURE 6: Overlay of experimental and back-calculated NOESY spectra for $(\mathbf{1})_2$. The experimental spectrum was acquired at 800 MHz in phosphate buffered saline at 288 K with 300 ms mixing time. The back-calculated spectra were generated based on pdb files of low energy structures using GIFA. (*29*). Signals from the experimental spectrum are shown in black, and those of the back calculated spectra are in green (major conformation) and blue (minor conformation).

NOESY spectra, and no structures were obtained that showed intercalation of the stilbene during the refinement phase. The overlay of the experimental and back-calculated NOESY spectra (Figure 6) was satisfactory only when back-calculated peaks from both conformations were included, strongly supporting that the two conformations are indeed resulting from the two different orientations of the stilbene relative to the neighboring nucleobases. The remaining discrepancies between experimental and back-calculated structures are to be expected when using the two-spin approximation for back-calculations and is within the range of what was observed in similar complexes that adopt a single conformation (*5*, *6*, *30*).

Structural details of the arrangement of the terminal residues in either conformation are shown in Figure 7. The 180° flip of the stilbene ring system between the two conformations slightly affects stacking between the nucleobase of T2 and the proximal benzene ring of TMS1, which is slightly more extensive in conformation 1, although stacking between this part of the hydrocarbon part of the ligand and the heterocycle are evident for both conformations. Interestingly, the distal ring of TMS1 does not fully cover the adenine nucleobase of A7. Instead, part of this benzene ring is above the minor groove, thus placing the middle methoxy group in a position where, together with the methoxy substituent facing the major groove, it can "embrace" the 2′-methylene group of the deoxyribose ring

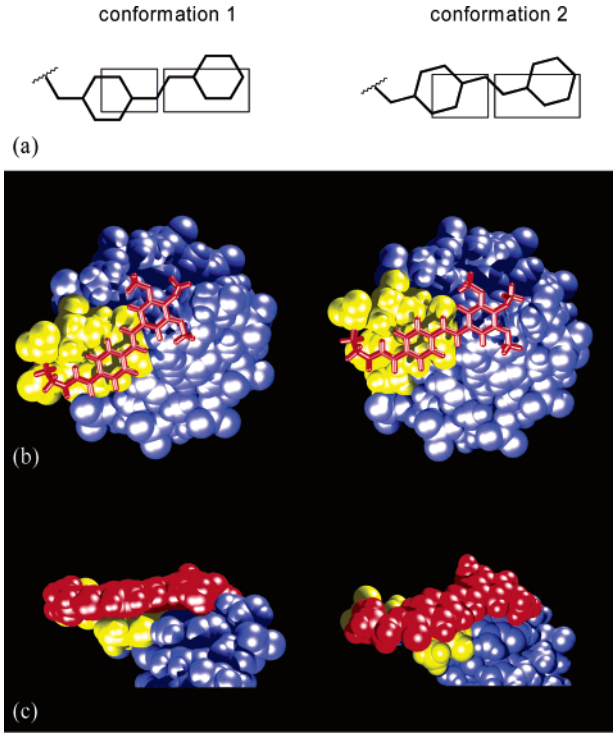

FIGURE 7: Two conformations of $(\mathbf{1})_2$, differing in the orientation of the stilbene ring relative to the DNA duplex. Left hand side: major conformation; right-hand side: minor conformation. (a) Cartoons showing the orientation of the stilbene; (b) and (c) low energy conformations obtained by restrained molecular dynamics. (b) View from the top with the stilbene displayed as a "licorice" and the remainder of the in space-filling represenation; (c) view perpendicular to the helical axis with all residues in space-filling representation. Color code for (b) and (c): stilbene substituent, red; 5′-terminal thymidine residue, yellow; remainder of the DNA, blue.

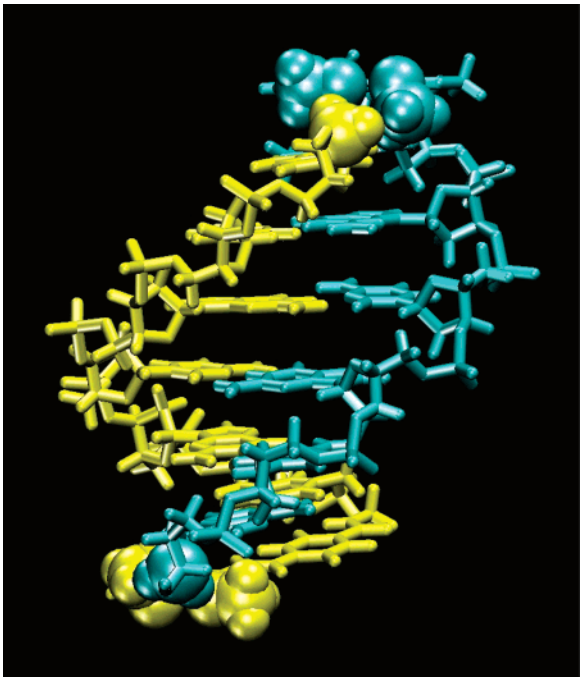

FIGURE 8: Embracing interactions between two methoxy groups of the stilbene moiety and the 2′-methylene group of the 3′-terminal residue A7. The structure shows the -OCH_3 groups of the ligand and the -CH_2- group of the deoxynucleoside in space filling representation and the remainder of the duplex in bond line representation to highlight the interaction partners. Strand A is in yellow, and strand B is in cyan. The drawing was generated from the major conformation using VMD.

of A7 (Figure 8). The embracing interaction is found in both conformations and seems to be adopted at the expense of more extensive stacking interactions between the aromatic rings of TMS1 and A7.

The methyl groups at position 5 of T2 and the edge of TMS1 that faces the minor groove protrude from the plane of the aromatic rings they are attached to. They thus presumably act as "stoppers" and aid the embracing methoxy groups in preventing sliding of the stilbene substituent on the base pair. The propyl linker between the carboxamide functionality of the stilbene and the 5′-phosphate group of T2 is long enough to allow for the stacking arrangement between the aromatic rings but does not have unnecessary "slack" that would make parts of it more solvent accessible and the ligand entropically more costly to engage in complex formation. Thus, the linker length, which is identical to that used in hairpin-bridging stilbenes (*11*), appears well optimized for the capping mode of binding of our ligand, which is linked to one terminus only. Overall, the folded structure $(\mathbf{1})_2$ adopts in either conformation is tight, without exposed loops. When viewed as a whole (Figure S4, Supporting Information), the stilbene appears as a "natural" extension of the π-stack of the helix.

DISCUSSION

The solution structures of stilbene-capped $(\mathbf{1})_2$ show capping and not intercalation of the tethered ligand. Figure S5 (Supporting Information) shows the terminus of a DNA duplex where the stilbene ring system is intercalating, which was obtained using selected constraints that favor a location between the terminal and penultimate base pair during restrained molecular dynamics. This structure shows that although intercalation is geometrically feasible, it may be unfavorable for the terminal base pair, whose thymine ring is not coplanar with A7. Typical intercalators, such as ethidium ions, acridine, or proflavine, have at least a tricyclic core system that provides a sufficiently large foundation for a neighboring base pair to stack on. In the trimethoxystilbene, the two rings are separated by a vinylic bridge, which offers very limited surface area for stacking.

In the structures obtained (Figure 7), the trimethoxybenzene ring of TMS1 does not seek maximum stacking overlap. Instead, it is found in a stacked arrangement that one might call "tiling", where only a portion of the aromatic ring systems of ligand and the nucleobase of A7 overlap. Apparently, the decisive interaction is between two of the methoxy groups, which form a cleft, and the methylene group at the 2′-position of the deoxyadenosine residue at the 3′-terminus. Which pair of methoxy group engages in this embracing interaction differs between the two conformations observed, but the binding mode is similar. Apparently, the protuberances above the plane of the terminal base pair that the 2′-methylenes of the deoxyribose residues constitute are an important feature of the binding surface. They can anchor the ligand and provide the side-on contacts that complement the face-on interactions that π-stacking provides.

The interactions observed thus confirm the expectation that the electron-rich trimethoxybenzene moiety does not seek optimal stacking interactions with the electron-rich adenine

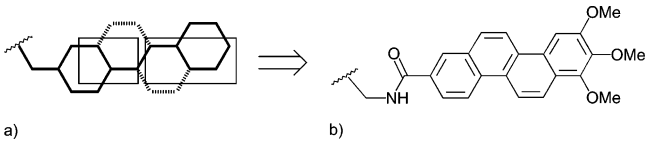

FIGURE 9: Proposed structure of further improved ligand for capping. (a) Cartoon of the expanded stilbene stacking on the terminal base pair (shown as rectangles). The benzannelations to be added to the stilbene ring system to enhance stacking with the terminal base pair are shown as broken lines. (b) Structure of proposed trimethoxychrysene substituent as a possible realization of a ligand with enhanced stacking capabilities.

ring system. Instead, interactions that involve the methyl groups of the methoxy substituents and the deoxyribose seem to dominate the interactions. The most distal methoxy group also engages in interactions with the CH-fragment at the 1′-position of the deoxyribose of A7. To do so, it partly "sinks" into the minor groove. The interactions of the methoxy groups thus ensure the tight fit that allows gauging the size and geometry of the terminal base pair. The tight fit explains the strong fidelity-enhancing effect that this substituent has on hybridization probes when forming base pairs at the terminus (*16*). The slow interconversion between the two conformations on the NMR time scale, which are probably due to a slow "off-rate" for the intramolecular release of the tightly bound stilbene, confirms that the aggregate strength of the interactions is very substantial.

Further support for the importance of the alkoxy groups in the stability of the complex between cap and DNA comes from the observation that a stilbene substituent lacking the methoxy group is less duplex stabilizing (*16*). The same is true for di- and pentafluorostilbene substituents, whose benzene rings are electron depleted and might engage in "donor−acceptor"-type stacking interactions. Stacking interactions between methyl groups and nucleobases are also known from the structure of a cholic acid-capped DNA duplex (*6*). How strong they can be has been shown in physical organic studies (*31*). Taken together, the evidence now suggests that for the capping mode of binding the aromatic moieties are entities that do not necessarily seek maximum π-stacking. They may act simply as rigid scaffolds that make possible other interactions and only stack to avoid exposure of hydrophobic surfaces to water. This view is confirmed by the edge-to-face arrangement between doubly tethered stilbenes and terminal base pairs in the recent high-resolution X-ray crystal structure of a hairpin (*3*).

Still, if one wanted to think of ways to improve π-stacking interactions, the present structure suggests a way to generate them. Figure 9 shows how one might expand the stilbene ring system to a chrysene, whose additional two benz-annelated rings can more extensively stack with the nucleobases without losing the grip of the methoxy groups on the 3′-terminal nucleotide.[2] The synthesis of a DNA strand with the ligand shown in Figure 9b as 5′-substituent should be within the realm of today's synthetic organic chemistry. Whether this expanded ligand will indeed be an even better cap or will find intercalation energetically more favorable to bury both of its π-surfaces is a question that deserves to be addressed experimentally. Perhaps further surprises are in store. After all, a small bicyclic heterocycle can also make the terminus of a DNA duplex refold (*30*).

Better understanding the binding properties and folding variants of termini should be worthwhile, given their importance for biochemical processes, such as those catalyzed by polymerases, repair enzymes, and gyrases. Mimicking interactions between termini and proteins with small molecules may also lead to new applications. Tethered ligands have been shown to be modulators of the rate and fidelity of nonenzymatic, template-directed primer extension reactions (*32*). Primer extension is a key technique in SNP genotyping (*33*). Another protein−DNA interaction that involves the termini that has recently come into focus is the gauging of the size of siRNA duplexes (*34*). Tryptophan residues were found to provide key stacking interactions, and mimicking them may lead to small ligands for monitoring the appearance of RNA species formed in RNA interference pathways. Melting curve studies have shown, however, that there can be substantial changes in the stabilizing effect of molecular caps on duplexes when the target strands are RNA rather than DNA (*8*).

As mentioned above, ligands tethered to termini can also enhance the target affinity and selectivity of hybridization probes, including those immobilized on microarrays (*16*). Their effect is not limited to blunt ends, as experiments with target strands with overhangs show (*16*). The present study shows that such ligands can gauge the size and identity of the terminal base pair by embracing the 3′-terminal nucleotide. These "read-out" interactions may be combined with contacts to the universal hydrogen bond acceptors (*O*2 of pyrimidines and *N*3 of purines) located in the minor groove (*35*). Tethered minor groove benders could provide these contacts. They are a class of fidelity-enhancing elements successfully applied in earlier studies (*9*). Finally, fundamental studies, such as those on electron transfer (*11*−*13*) may benefit from structurally defined arrangements between ligands and duplexes. The current structure shows how such arrangements may be created, starting from singly tethered stilbenes.

ACKNOWLEDGMENT

Expert technical assistance by Annette Hochgesand during the synthesis of **1** is gratefully acknowledged. The authors thank A. Friemel (U. Konstanz) for help with the acquisition of exploratory NMR spectra and Prof. C. Griesinger for making available resources at the Max-Planck-Institute in Göttingen.

SUPPORTING INFORMATION AVAILABLE

Mass spectrum, UV spectrum, and structural drawing with naming scheme for **1**, stereoview of $(\mathbf{1})_2$, view of a terminus with intercalated stilbene, chemical shift assignments, and helical parameters for the two predominant conformations of $(\mathbf{1})_2$. This material is available free of charge via the Internet at http://pubs.acs.org.

REFERENCES

1. Blackburn, G. M., and Gait, M. J. (1996) *Nucleic Acids in Chemistry and Biology*, 2nd ed., pp 329−374, Oxford University Press, Oxford.

[2] We are grateful to one of the referees for pointing out that a chrysene may lack the flexibility of our stilbene, possibly making it more difficult to fit tightly to the surface of the terminal base pair.

2. Lewis, F. D., Liu, X., Wu, Y., Miller, S. E., Wasielewski, M. R., Letsinger, R. L., Sanishivili, R., Joachimiak, A., Tereshko, V., and Egli, M. (1999) Structure and photoinduced electron transfer in exceptionally stable synthetic DNA hairpins with stilbenediether linkers, *J. Am. Chem. Soc. 121*, 9905−9906.
3. Egli, M., Tereshko, V., Mushudov, G. N., Sanishvili, R., Liu, X., and Lewis, F. D. (2003) Face-to-face and edge-to-face $\pi-\pi$ interactions in a synthetic DNA hairpin with a stilbenediether linker, *J. Am. Chem. Soc. 125*, 10842−10849.
4. Maltseva, T. V., Agback, P., Repkova, M. N., Venyaminova, A. G., Ivanova, E. M., Sandtrom, A., Zarytova, V. F., and Chattopadhyaya, J. (1994) The solution structure of a 3′-phenazinium (Pzn) tethered DNA-RNA duplex with a dangling adenosine: r(5′G-AUUGAA3′): d(5′TCAATC3′-Pzn), *Nucleic Acids Res. 22*, 5590−5599.
5. Ho, W. C., Steinbeck, C., and Richert, C. (1999) Solution structure of the aminoacyl-capped oligodeoxyribonucleotide duplex (W-TGCGCAC)$_2$, *Biochemistry 38*, 12597−12606.
6. Tuma, J., and Richert, C. (2003) Solution structure of a steroid-DNA complex with cholic acid residues sealing the termini of a Watson−Crick duplex, *Biochemistry 42*, 8957−8965.
7. Hunter, C. A., and Sanders, J. K. M. (1990) The nature of $\pi-\pi$ interactions, *J. Am. Chem. Soc. 112*, 5525−5534.
8. Bleczinski, C. F., and Richert, C. (1999) Steroid-DNA interactions increasing stability, sequence-selectivity, DNA/RNA discrimination, and hypochromicity of oligonucleotide duplexes, *J. Am. Chem. Soc. 121*, 10889−10894.
9. Kutyavin, I. V., Afonina, I. A., Mills, A., Gorn, V. V., Lukhtanov, E. A., Belousov, E. S., Singer, M. J., Walburger, D. K., Lokhov, S. G., Gall, A. A., Dempcy, R., Reed, M. W., Meyer, R. B., and Hedgpeth, J. (2000) 3′-minor groove binder-DNA probes increase sequence specificity at PCR extension temperatures, *Nucleic Acids Res. 28*, 655−661.
10. Narayanan, S., Gall, J., and Richert, C. (2004) Clamping down on weak terminal base pairs: oligonucleotides with molecular caps as fidelity-enhancing elements at the 5′- and 3′-terminal residues, *Nucleic Acids Res. 32*, 2901−2911 and references therein.
11. Lewis, F. D., Wu, T., Zhang, Y., Letsinger, R. L., Greenfield, S. R., and Wasielewski, M. R. (1997) Distance-dependent electron transfer in DNA hairpins, *Science 277*, 673−676.
12. Lewis, F. D., Liu, X., Liu, J., Miller, S. E., Hayes, R. T., and Wasielewski, M. R. (2000) Dynamics of hole hopping in DNA, *Nature 406*, 51−53.
13. Lewis, F. D., Wu, Y. S., and Liu, X. Y. (2002) Synthesis, structure, and photochemistry of exceptionally stable synthetic DNA hairpins with stilbene diether linkers, *J. Am. Chem. Soc. 124*, 12165−12173.
14. Festy, B., and Daune, M. (1973) Hydroxystilbamidine. Nonintercalating drug as a probe of nucleic acid conformation, *Biochemistry 12*, 4827−4834.
15. Fukuhara, K., and Miyata, N. (1998) Resveratrol as a new type of DNA-cleaving agent, *Bioorg. Med. Chem. Lett. 8*, 3187−3192.
16. Dogan, Z., Paulini, R., Rojas Stütz, J. A., Narayanan, S., and Richert, C. (2004) 5′-Tethered stilbene derivatives as fidelity- and affinity-enhancing modulators of DNA duplex stability, *J. Am. Chem. Soc. 126*, 4762−4763.
17. Sklenar, V., Piotto, M., Leppik, R., and Saudek, V. (1993) Gradient tailored water suppression for ^{1}H-^{15}N HSQC experiments optimized to retain full sensitivity, *J. Magn. Res. Ser. A 102*, 241−245.
18. Scheek, R. M., Boelens, R., Russo, N., van Boom, J. H., and Kaptein, R. (1984) Sequential resonance assignments in proton NMR spectra of oligonucleotides by two-dimensional NMR spectroscopy, *Biochemistry 23*, 1371−1376.
19. Feigon, J., Leupin, W., Denny, W. A., and Kearns, D. R. (1983) Two-dimensional proton nuclear magnetic resonance investigation of the synthetic deoxyribonucleic acid decamer d(ATATC-GATAT), *Biochemistry 22*, 5943−5951.
20. Patel, D. J., Shapiro, L., and Hare, D. (1986) Sequence-dependent conformation of DNA duplexes. The AATT segment of the d(G-G-A-A-T-T-C-C) duplex in aqueous solution, *J. Biol. Chem. 261*, 1223−1229.
21. X-PLOR, version 3.1, A. T. Brünger, X-PLOR Manual, Yale University Press (1992), Yale University, New Haven, CT.
22. Brünger, A. T., Adams, P. D., Clore, G. M., DeLano, W. L., Gros, P., Grosse-Kunstleve, R. W., Jiang, J.-S., Kuszewski, J., Nilges, N., Pannu, N. S., Read, R. J., Rice, L. M., Simonson, T., and Warren, G. L. (1998) Crystallography & NMR system (CNS): a new software system for macromolecular structure determination, *Acta Crystallogr. D54*, 905−921.
23. Wijmenga, S. S., Mooren, M. M. W., and Hilbers, C. W. (1993) in *NMR of Macromolecules, A Practical Approach* (Roberts, G. C. K., Ed.) pp 217−288, Oxford University Press, Oxford, UK.
24. Saenger, W. (1984) *Principles of Nucleic Acid Structure*, Springer, New York.
25. Kleywegt, G. J., and Jones T. A. (1997) Model-building and refinement practice, *Methods Enzymol. 277*, 208−230.
26. Stalmach, U., Schollmeyer, D., and Meier, H. (1999) Single-crystal structures of model compounds for poly(2,5-dialkoxy-1,4-phenylenevinylene), *Chem. Mater. 11*, 2103-2106.
27. Stein, E. G., Rice, L. M., and Brünger, A. T. (1997) Torsion angle molecular dynamics: a new, efficient tool for NMR structure elucidation, *J. Magn. Res. Ser. B*, *124*, 154−164.
28. Schwieters, C. D., and Clore, G. M. (2001) The VMD-XPLOR visualization package for NMR structure refinement, *J. Magn. Res. 149*, 239−244.
29. Pons, J. L., Malliavin, T. E., and Delsuc, M. A. (1996) Gifa V4: a complete package for NMR data-set processing, *J. Biomol. NMR, 8*, 445−452.
30. Tuma, J., Connors, W. H., Stitelman, D. H., and Richert, C. (2002) On the effect of covalently appended quinolones on termini of DNA-duplexes, *J. Am. Chem. Soc. 124*, 4236−4246.
31. Kim E.-i., Paliwal, S., and Wilcox, C. S. (1998) Measurement of molecular electrostatic field effects in edge-to-face aromatic interactions and CH-π interactions with implications for protein folding and molecular recognition, *J. Am. Chem. Soc. 120*, 11192−11193.
32. Rojas Stütz, J. A., and Richert, C. (2001) A steroid cap induces enhanced selectivity and rates in nonenzymatic single nucleotide extensions of an oligonucleotide, *J. Am. Chem. Soc. 123*, 12718−12719.
33. Tost, J., and Gut, I. G. (2002) Genotyping single nucleotide polymorphisms by mass spectrometry, *Mass Spectrom. Rev. 21*, 388−418.
34. Ye, K., Malinina, L., and Patel, D. J. (2003) Recognition of small interfering RNA by a viral suppressor of RNA silencing, *Nature 426*, 874−878.
35. Seeman, N. C., Rosenberg, J. M., and Rich, A. (1976) Sequence-specific recognition of double helical nucleic acids by proteins, *Proc. Natl. Acad. Sci. U.S.A. 73*, 804−808.

BI048205Y